



UDC 544. 653.2

## ***In-silico* STUDY OF ANTHRAQUINONE DERIVATIVES AS PROBABLE INHIBITORS OF COVID-19**

Vasyl I. Shupeniuk<sup>1\*</sup>, Amaladoss Nepolraj<sup>2</sup>, Tatiana N. Taras<sup>1</sup>, Oksana P. Sabadakh<sup>1</sup>,  
Mykola P. Matkivskiy<sup>1</sup>, Yevhen R. Luchkevych<sup>1</sup>

<sup>1</sup>Department of the Environment and Chemical Education, Vasyl Stefanyk Precarpathian National University, Shevchenko Street 57, Ivano-Frankivsk 76018, Ukraine

<sup>2</sup>Department of Chemistry, Annai College of Arts and Science, Kovilacheri, Kumbakonam, Tamilnadu 612503, India  
Received 20 November 2021; accepted 1 July 2022; Available online 25 July 2022

### Abstract

Five previously known anthraquinones with amino derivatives and synthesized new triazene (1-[(1E)-3,3-bis(2-hydroxyethyl)triaz-1-en-1-ol]-4-[(2-hydroxyethyl)amino]anthracene-9,10-dione) were evaluated *in-silico* as inhibitors of COVID-19 main protease. Preliminary screening has shown that the presence of a sulfo group in the second position of the anthraquinone ring reduces activity, probably due to the inability of the molecule to cross the hydrophilic-lipophilic barrier. Therefore, the desulfation reaction of 4-substituted anthraquinone was carried out and triazene was synthesized on its basis, which due to the presence of a triazene bridge showed good activity. The structures of the synthesized compound were confirmed by IR, <sup>1</sup>H, <sup>13</sup>C NMR, and LC-MS spectral studies. Chemo-informatics study showed that the compound obeyed the Lipinski's rule. Computational docking analysis was performed using PyRx, AutoDock Vina option based on scoring functions. *In-silico* molecular docking study results demonstrated greater binding energy and affinity to the active binding site of the N3 Coronavirus primary protease.  
**Keywords:** Anthraquinones; triazene; molecular docking; RNA polymerase; protease Covid-19.

## ***In-silico* ДОСЛІДЖЕННЯ ПОХІДНИХ АНТРАХІНОНУ ЯК МОЖЛИВИХ ІНГІБІТОРІВ COVID-19**

Василь І. Шупенюк<sup>1</sup>, Амаладосс Неполрай<sup>2</sup>, Тетяна Н. Тарас<sup>1</sup>, Оксана П. Сабадах<sup>1</sup>,  
Микола П. Матківський<sup>1</sup>, Євген Р. Лучкевич<sup>1</sup>

<sup>1</sup>Прикарпатський національний університет імені Василя Стефаника, вул. Шевченко, 57, Івано-Франківськ, 76018, Україна

<sup>2</sup>Аннаїський коледж мистецтв та наук, Ковилачері, Кумбаконам, Тамилнаду 612503, Індія

### Анотація

П'ять раніше відомих антрахінонів з амінопохідними та синтезований новий триазен (1-[(1E)-3,3-біс(2-гідроксиетил)триаз-1-ен-1-ол]-4-[(2-гідроксиетил)аміно]антрацен-9,10-діон) оцінювали *in-silico* як потенційних інгібіторів основної протеази COVID-19. Попередній скринінг виявив, що наявність сульфогрупи в другому положенні антрахінонового кільця зменшує активність ймовірно через нездатність молекули пройти через гідрофільно-ліпофільний бар'єр. Тому проведено реакцію десульфування 4-заміщеного антрахінону і на його основі синтезовано триазен, який завдяки наявності триазенового містка проявив хорошу активність. Структури синтезованої сполуки підтверджено ІЧ, <sup>1</sup>H, <sup>13</sup>C ЯМР та LC-MS спектральними дослідженнями. Хіміко-інформаційне дослідження показало, що сполука підкорялася правилу Ліпінського. Обчислювальний аналіз *in-silico* проводився з використанням PyRx, параметра AutoDock Vina на основі функцій оцінки. Результати дослідження молекулярного докінгу продемонстрували більшу енергію зв'язування та спорідненість з активним ділянкою зв'язування N3 первинної протеази коронавірусу.

Ключові слова: Антрахінони; триазен; молекулярний докінг; РНК-полімераза; протеаза Covid-19.

\*Corresponding author: e-mail address: vasyi.shupeniuk@pnu.edu.ua

© 2022 Oles Honchar Dnipro National University;

doi: 10.15421/jchemtech.v30i2.244728

## Introduction

Coronavirus disease stated December 2019 in Wuhan, China [1]. The epidemic was isolated to a new type strain of coronavirus, the name of which given by the World Health Organization (WHO) was 2019-nCoV or COVID-19 [2]. Coronaviruses contain a positive-sense with single-stranded RNA genome [3]. The genome size of coronaviruses ranges from 26.4 to 31.7 kilobases genome size is one of significant between RNA viruses. Recent studies suggested that human COVID-19 is a valid target for antiviral drug development based on this aspect, a structure-based virtual screening approach to target the nucleocapsid protein. The success of a drug entrant is resolute not only by its most readily useful potential, but in addition to a satisfactory analysis that is ADME that predict of some important capacity to properties in-silico, and it is valuable for analysis regarding the excellent qualities of the molecules [4].

Antraquinones compounds are greatest known for their various biological activities [5]. They have successfully treated many diseases such as cancer and malaria [6]. At present, anthraquinone derivatives are extensively studied as therapeutic agents against COVID-19 [7]. In this research paper, anthraquinones compounds has been evaluated for their potential anti-COVID-19 activity and explored through in-silico molecular docking studies. Molecular docking for the total most part used approach in structure-based drug design. The synthesized compound of ligand was drawn with Chem Draw Ultra version 16.0 (Cambridge Software) followed by resulting molecular mechanics (MM2) energy minimization of ligands using ChemBio-3D Ultra version 12.0. These energy - minimized ligands (structures) MOL, SDF format of that ligands had been converted to mol2 file using open Babel and Discovery studio tool and ligand preparation was done using the Chimera software ended up being used in molecular docking study [8]. The results of docking by using AutoDock4 were first converted to \*.pdbqt. Docking was done with a Lamarckian genetic algorithm and default parameters. The grid box size was set at 40 Å for x, y and z respectively, and the grid center was set to -11.183, 10.406 and 68.139 for x, y and z respectively, which covered all the amino acid. The spacing between grid points was 0.514 angstroms. The first ten top-ranked docking poses were saved for each docking run. To approve the molecular docking protocol, the corresponding reference ligands

(sulfite, triazene) were initially docked into the crystal structure.

## Materials and methods

### Chemistry

All chemicals were obtained from commercial sources and used without further purification. Melting points were measured in open capillary tubes. <sup>1</sup>H NMR spectra were recorded on a Varian 400 spectrometer at 400 MHz using DMSO-d<sub>6</sub> as solvent unless otherwise noted. Mass spectra were determined on an Agilent 1100 Series high-performance liquid chromatograph equipped with a diode detector and an Agilent mass-selective detector with the ability to quickly switch between positive and negative ionization modes. The course of the reactions was monitored by TLC on silica gel plates DC-Fertigfolien Alugram Xtra Sil G/UV254 (Germany).

*1-Amino-4-[(2-hydroxyethyl)-amino]anthracen-9,10-dione* (7). Compound **6** (0.01 mol) was dissolved in 150 ml of hot water and Na<sub>2</sub>S<sub>2</sub>O<sub>4</sub> (0.1 mol) was added. Then the temperature of the reaction mixture was gradually raised to 60–90 °C. The reaction proceeded for 5 hours, the precipitate was filtered off on a Buchner funnel, squeezed thoroughly, and washed with 10 ml of 30 % NaCl solution.

Yield – 88 %. Chromato-mass spectrum: *m/z*: 283.2 [M]<sup>+</sup>; C<sub>16</sub>H<sub>14</sub>N<sub>2</sub>O<sub>3</sub>; calculated *m/z*: 283. <sup>1</sup>H NMR (DMSO-*d*<sub>6</sub>) δ: 3.49 - 3.50 m (2H, CH<sub>2</sub>), 3.68 t (2H, CH<sub>2</sub>), 7.31 - 7.38 m (2H, OH, NH<sub>2</sub>), 7.76 t (2H, H<sup>2,4</sup>), 8.23 - 8.34 m (4H, H<sub>arom.</sub>), 10.87 - 10.88 m (1H, NH). Found: % C 67.13; H 3.97; N 10.89; S 0.4 C<sub>16</sub>H<sub>13</sub>N<sub>2</sub>O<sub>3</sub>. Calculated, %: C 67.9; H 4.63; N 9.89.

*1-(Diazyn-1-ium-1-yl)-4-[(2-hydroxyethyl)-amino]anthracene-9,10-dione* (8). A 50-mL round-bottom flask equipped with a magnetic stirrer was charged with a solution of anthraquinone **7** (0.1 mmol) in 1 M aqueous HCl (5.0 mL). The solution was cooled to 0–5 °C in an ice bath, a solution of sodium nitrite (0.2 mmol) in 0.5 mL of distilled water was added dropwise, maintaining the temperature at 0–5 °C, and the mixture was stirred for 5 min at that temperature.

*Triazene derivative 9*. The mixture containing diazonium salt **8** was allowed to warm up to room temperature, a solution of the corresponding amine (0.15 mmol) in 5 mL of ethanol was added, and the mixture was stirred for ~30 s at room temperature. The course of the reaction was monitored by the color change of the reaction mixture (after diazotization, the color changed from blue to red), as well as by the

TLC method using acetone–water (2 : 3) as an eluent. The product was purified by reverse phase column chromatography (RP-18) using water as eluent to a yellow crystalline solid, 61 % yield;

IR (KBr,  $\nu_{\max}$ ,  $\text{cm}^{-1}$ ): 3488, 2949, 1693, 1668, 1598, 1589, 1420.  $^1\text{H}$  NMR (400 MHz, DMSO- $d_6$ ):  $\delta$  3.00 t (4H,  $\text{CH}_2$ ), 3.38 – 3.42 t (4H,  $\text{CH}_2$ ), 3.65 t (4H,  $\text{CH}_2$ ), 5.08 s (1H, OH), 5.25 s (2H, OH), 7.85 – 7.90 m (2H,  $\text{H}_{\text{arom.}}$ ), 8.13 – 8.15 m (2H,  $\text{H}_{\text{arom.}}$ ), 8.69 s (2H,  $\text{H}_{\text{arom.}}$ ), 9.88 s (1H, NH).  $^{13}\text{C}$  NMR (100 MHz, DMSO- $d_6$ )  $\delta$  45.35, 55.70, 59.60, 60.40 ( $\text{CH}_2$ ); 122.58, 124.42, 127.11, 127.21, 127.40, 131.71, 133.22, 134.83, 135.58, 136.29, 140.89, 152.98 ( $\text{C}_{\text{ar}}$ ); 180.82, 181.09 ( $\text{C}=\text{O}$ ). LC-MS:  $m/z$  588.0  $[\text{M}+\text{H}]^+$ .

### Pharmacological/biological assays

**ADME analysis.** ADME analysis was performed using SWISS ADME and the Molinspiration predictor for the current study. This web server acts as a tool to evaluate ADMET properties such as molecular weight < 500, number of bonds < 10, rotatable bonds, hydrogen bond acceptor, hydrogen bond donor (HBDs), molar refractivity, topological polar surface area (TPSA), water solubility (logS), blood brain-barrier, skin permeability (logKp), synthetic accessibility score (SA), percentage absorption, pharmacokinetics, drug-lead likeness and medicinal chemistry friendliness properties of drug molecules. The lipophilicity of the molecules was obtained by integrating the analysis results from several log P prediction programs such as iLOGP, XLOGP3, WLOGP, MLOGP and SILICOS-IT. The lipophilicity fraction of a molecule is the log ratio of the concentration of the drug substance in the two solvents in the unified form, the lower the log P value, the stronger the lipophilicity. The log S distribution between -1 and -4 will be improved for better absorption and distribution of drugs in the form [9].

### Molecular docking

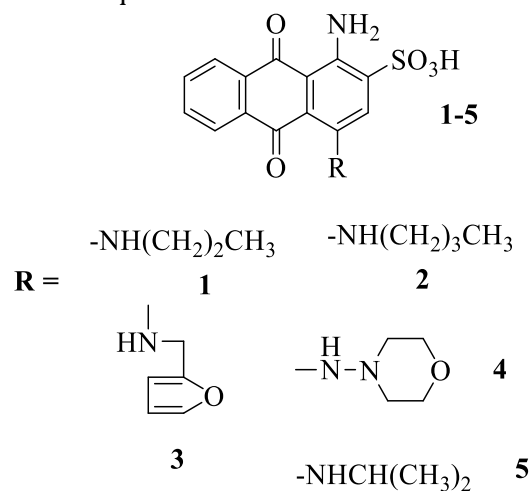
The crystal structure of 3CLpro-2 (PDB code: 6LU7) [10], was obtained via Protein Data Bank (<http://www.pdb.org>) and any heteroatoms (in particular, furan, not to interfere with determination), and water molecules were eliminated for molecular docking studies. Molecular docking was performed using the Autodock Tools 1.5.4 package (<http://mgltools.scripps.edu>) [11] as well as Autodock Vina (version 4.2 docking programs) and SAMSON (extended docking programs). The

values of the grid box parameters in the VINA search space derived from a single calculation ( $X = 10.711$ ,  $Y = 12.411$  and  $Z = 68.83$ ) had been adjusted using the default exhaustiveness value = 8 to maximize binding conformational analysis. The generated docked complexes were evaluated based on the lowest binding energy (kcal/mol) taken from the literature [10–12], values and structure-activity relationship (SAR) analysis, which showed the clear presence of hydrogen bonding, hydrophobic interaction between ligand compound and good control of each of the receptors that were focused on. 3D and 2D graphical images of all docked complexes were performed using UCSF Chimera 1.10.1, Discovery Studio (2.1.0), PyMOL software and an online web server (<https://proteins.plus/>) [13].

## Results and discussion

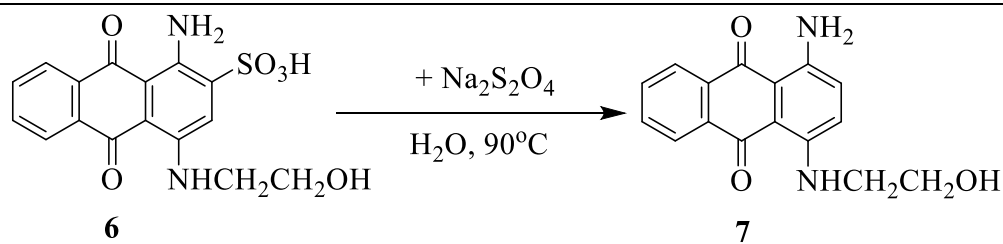
### Chemistry

Screening (molecular docking) of 4-substituted derivatives based on bromamic acid synthesized and described by us earlier (Scheme 1) [14–15] did not show high activity, so we decided to remove the sulfo group molecule from anthraquinone.



**Scheme 1:** Anthraquinone compounds

Reactions in which the sulfogroup of bromamic acid enters are described in the literature. This is chlorination followed by substitution of chlorine for aromatic amine derivatives. With this reaction, the authors [16] obtained a promising class of ectonucleoside inhibitors – NTPDases. It is known that the sulfo group is capable of entering into complexes with metals and cations of amino derivatives. The method of desulfurization of 4-substituted anthraquinone-2-sulfonic acids is described. In our case, a strong reducing agent sodium dithionate was used to remove the sulfo group from the molecules of compound 6:

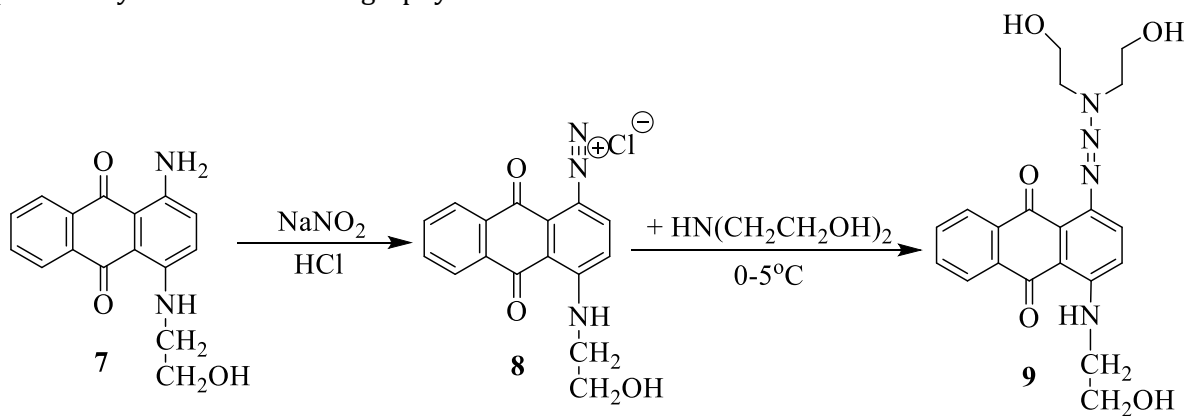


88 % (m/z [M + Z]<sup>+</sup> 283,2)

The formation of the desulfurization product 7 is fully confirmed by the chromatato-mass spectrum and elemental analysis. Thus, in the NMR-1H spectrum of compound 7 protons of methylene groups are present at 3.50 ppm and 3.68 ppm, there are also shifts of 6 aromatic protons at 7.38 ppm and 8.23–8.34 ppm, and a multiplet of the NH group at 10.80 ppm. The absence of sulfogroups was determined by the negative reaction to NaOH. The planned triazene compound, which could be highly active, was synthesized in two stages. Aminoanthraquinone 7 was subjected to diazotization with sodium nitrite in an aqueous medium in the presence of HCl at 0–5 °C [17]. The subsequent azo coupling of the diazonium salt 8 with a secondary amine led to the formation of triazene 9. After the usual aqueous treatment, the condensed residue [18] was purified by column chromatography on silica

gel to obtain a light yellow acicular crystal with a yield of 61 %.

The prominent absorption bands in IR spectrum appeared at 3488 cm<sup>-1</sup> due to the (-OH stretching), 2949 cm<sup>-1</sup> (-CH<sub>2</sub>-stretching), 1589 cm<sup>-1</sup> (C=H of aromatic ring), 1668 (C=C stretching of aromatic ring), 1693 cm<sup>-1</sup> due to ketone functional group stretching frequencies respectively, the bond at 1598 cm<sup>-1</sup> due to C-N group, presence of triazene confirmed peak 1420 cm<sup>-1</sup> (N=N). The <sup>1</sup>H NMR spectrum of 9 showed a downfield board singlet at δ 9.88 due to -NH protons. The aromatic protons appearing at δ 7.85–8.69, are due to anthraquinone ring, the <sup>13</sup>C NMR spectra unambiguously matched the structure of the corresponding 1-[(1E)-3,3-bis(2-hydroxyethyl)triaz-1-en-1-ol]-4-[(2-hydroxyethyl)amino]anthracene-9,10-dione 9.



### Pharmacology

The predicted chemo-informative properties were evaluated using in silico computational studies, which demonstrate that the compounds have promising drug-like properties. The results associated with the predictor values of SWISS ADME and Molinspiration log P and the molar refraction to the total polar surface area in these molecules were in excellent agreement with the most important rules of drug similarity. The results showed that compounds 1-5, 9 have ADME parameters of H-bond acceptor and H-donor, polar surface area and molar volume (figure 1 of compound 9, other compounds are listed in Supplementary Information). These

compounds have demonstrated stability, hydrophilicity, and lipophilicity, which makes them bioavailable. Molecules with TPSA > 134 are considered to have low oral bioavailability. The molecular polar surface area (PSA) is a very useful parameter for the transport properties of compounds. A molecule is clearly defined as the sum of the surface area of all polar atoms, primarily oxygen, nitrogen and attached hydrogen atoms. This parameter has been shown to correlate very well with human intestinal absorption, Caco-2 monolayer permeability, and blood-brain barrier penetration.

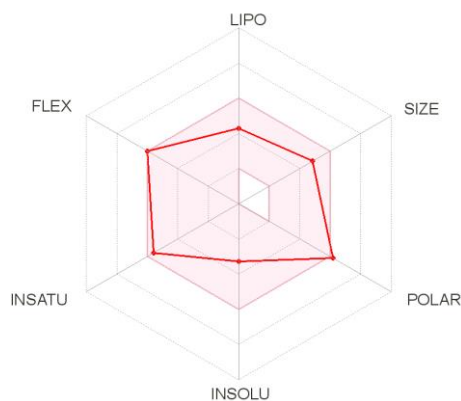


**Fig. 1.** Bioavailability radar graph of 1-[(1E)-3,3-bis(2-hydroxyethyl)triaz-1-en-1-ol]-4-[(2-hydroxyethyl)amino]anthracene-9,10-dione, (pink area reflects the allowed values of drug likeness properties of the molecule)

Checking for Lipinski's rule RO5 showed that compounds 1–5, 9 had good molecular weight

(g/mol), two values of allowable hydrogen bonds, and values of hydrogen bond donors log P 0.95–3.4, which confirms, that their behavior is similar to medicinal products. The results obtained from the Swiss search engine ADME and Mol inspiration are shown in Table 1.

The boiled-egg diagram analysis shows that the compounds are strong in the acceptable range of standard drugs, the blue dot indicates that the CNS P-glycoprotein system P-glycoprotein can not be affected, the dot located in the yolk of the boiled egg is a molecule passively penetrating the blood-brain barrier (BBB) ((Figure 2, compound 9, other compounds are listed in the Supplementary Information). In this study, the synthesized ligand and its complexes were found out to be in good compliance with the criteria and can be said to be bioavailable.

Table 1

Physicochemical descriptors and ADME parameters <sup>a</sup>						
parameters/compound	9	1	2	3	4	5
M.W, g/mol	398.41	360.38	374.41	398.39	403.41	360.38
RB	9	4	5	4	3	3
H-A	7	5	5	6	7	5
H-D	4	3	3	3	3	3
TPSA	134.82 Å <sup>2</sup>	134.94 Å <sup>2</sup>	134.94 Å <sup>2</sup>	148.08 Å <sup>2</sup>	147.41 Å <sup>2</sup>	134.94 Å <sup>2</sup>
MR	105.04	92.93	97.74	100.07	103.52	92.93
WlogP (lipophilicity)	0.96	3.01	3.4	3.24	1.47	3.01
ESOL logS	-3.29	-4	-4.23	-4.15	-2.21	-4.01
BBB Permeant	No	No	No	No	No	No
log K <sub>p</sub> cm <sup>-1</sup>	-7.3	-6.43	-6.26	-6.87	-9.04	-6.5
Lipinski violations	0	0	0	0	0	0
PAINS alerts	3	2	2	2	2	2
Synthesis Accessibility	3.67	3.19	3.26	3.29	3.54	3.22

<sup>a</sup>R bond =Rotatable bond, H-A = Hydrogen bond acceptor, H-D = hydrogen bond donor, TPSA = topological polar surface area, BBB = blood brain-barrier, log P = lipophilicity, log S = water solubility, log K<sub>p</sub> = permeability coefficient, PAINS = pan-assayinterference structure.

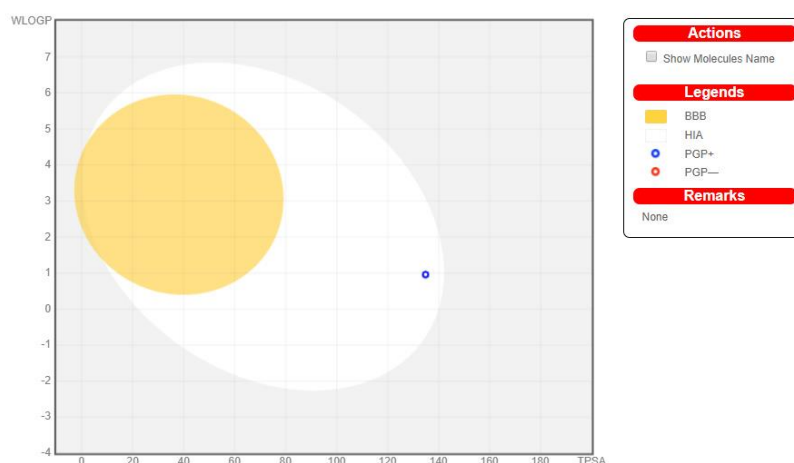


**Fig. 2:** ADME properties of compound 1-[(1E)-3,3-bis(2-hydroxyethyl)triaz-1-en-1-ol]-4-[(2-hydroxyethyl)amino]anthracene-9,10-dione by graphical representation (boiled-egg diagram)

### Molecular docking

The molecular docking method in medicinal chemistry has led to advances in drug discovery and development. This method investigates the binding method and affinity of a small molecule to the binding site of the target receptor protein. The docked ligands were ranked according to

their binding affinity in the ligand-receptor system (Figure 3). Molecular docking was performed for compound **9** against the main protease 3CLpro-2 (6LU7) to identify ligand-protein interactions

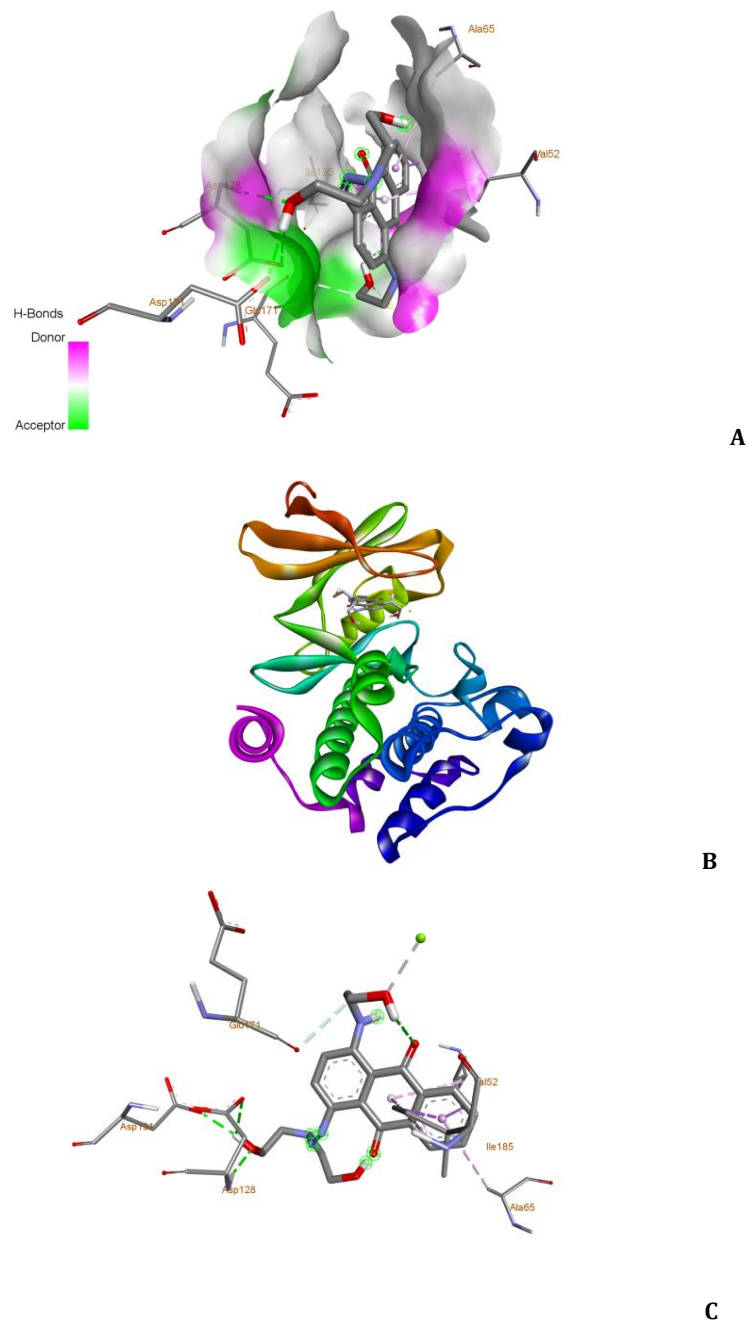


**Fig. 3. (A) H-bond surface interaction of the COVID-19 receptor inhibitor (B) with ligand 9. Docking of triazene ligand 9 to the same catalytic receptor site, (C). Compound 9 3D docking results at the N3 binding site of the main COVID-19 protease**

The docking result showed that six hydrogen bonds, one electrostatic bond, and one hydrophobic interaction were observed in the synthesized docking complex (Fig. 3 compound **9**, the remaining compounds are listed in the Supplementary Information). According to the

results obtained in Autodock Vina, it was decided that the docked ligand forms a stable complex with the COVID-19 inhibitor. Nine representative binding modes with affinities ranging from -8.2 to -7.2 kcal/mol were detected for triazene **9** (Table 3).

The binding affinity values of different poses of compound 1-[(1E)-3,3-bis(2-hydroxyethyl)triaz-1-en-1-ol]-4-[(2-hydroxyethyl)amino]anthracene-9,10-dione predicted with Autodock Vina

Mode	Affinity (kcal/mol)	Distance from the bestmode	
		RMSD1.b.	RMSD u.b.
1	-8.2	0.000	0.000
2	-7.8	2.452	4.321
3	-7.5	3.412	6.230
4	-7.7	2.513	3.505
5	-7.4	3.337	6.074
6	-7.4	3.079	6.000
7	-7.4	2.665	5.229
8	-7.2	2.703	5.348
9	-7.2	2.312	2.901

Molecular 2D docking of compound 9 in Fig. 4 showed binding of the amino acids-lysine to the hydroxyethylamine group, leucine to the

anthraquinone ring, and hydrogen bonding of glycine to hydroxy groups.

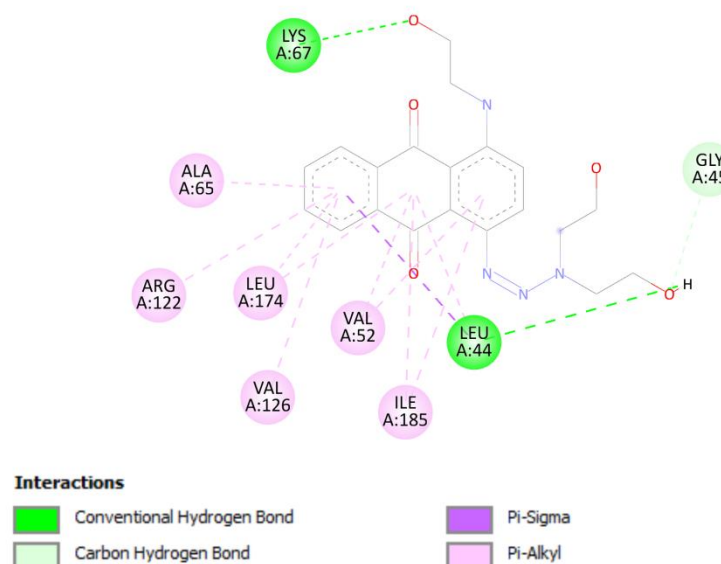


Fig. 4. (a) 2D H-bond surface interaction of COVID-19 receptor inhibitor with ligand 9, (b) 2D docking of compound 9 into the N3 binding site of the main COVID-19 protease

## Conclusion

An in-silico study of 4-substituted anthraquinone compounds was conducted for the first time. The results showed that the compounds inhibited and bound to the main protease (6LU7). Triazene 9, which lacked a sulfo group, showed the highest affinity (-7.8 kcal/mol in AutoDock 4 and -7.0 in AutoDock Wines). In fact, these results suggested that the

configuration of the binding site might have a favorable orientation. An in-silico ADME study that provided information on the toxicity and drug-likeness of compound 9 in particular, and its evaluation against anti-COVID-19 drugs, suggested that this compound was a promising source for the development of a selective, safe, and potent inhibitor of COVID-19.

## References

- [1] Zhu, N., Zhang, D., Wang, W., Li, X., Yang, B., Song, J., Zhao, X., Huang, B., Shi, W., Lu, R., Niu, P., Zhan, F., Ma, X., Wang, D., Xu, W., Wu, G., Gao, G. F., Tan W. A. (2019). Novel coronavirus from patients with pneumonia in China, *N. Engl. J. Med.*, 382(8), 727-733. doi: 10.1056/NEJMoa2001017
- [2] Wu, A., Peng, Y., Huang, B., Ding, X., Wang, X., Niu, P., Meng, J., Zhu, Z., Zhang, Wang, Z., Sheng, J., Quan, J. L., Xia, Z., Tan, W., Cheng, G., Jiang T. (2020). Genome Composition and Divergence of the novel coronavirus

- (2019-nCoV) originating in China, *Cell Host. Microbe.*, 27(3), 325–328. <https://doi.org/10.1016/j.chom.2020.02.001>
- [3] Fehr, A. R., Perlman, S. (2015). Coronaviruses: An overview of their replication and pathogenesis, *Methods. Mol. Biol.*, 1282, 1–23. [https://doi.org/10.1007/978-1-4939-2438-7\\_1](https://doi.org/10.1007/978-1-4939-2438-7_1)
- [4] Jamkhande, P. G., Pathan, S. K., Wadher, S. J. (2016). In silico PASS analysis and determination of antimycobacterial, antifungal, and antioxidant efficacies of maslinic acid in an extract rich in pentacyclic triterpenoids, *Int. J. Mycobacteriol.*, 5, 417–25. <https://doi.org/10.1016/j.ijmyco.2016.06.020>
- [5] Malik, E., Muller, C. (2016). Anthraquinones as pharmacological tools and drugs., *Med. Res. Rev.*, 36, 705. <https://doi.org/10.1002/med.21391>
- [6] Hussain, H., Al-Harrasi, A., Al-Rawahi, A., Green, I., Csuk, R., Ahmed, I., Shan, A., Abbas, G., Rehman, N., Ullah, R. (2015). A fruitful decade from 2005 to 2014 for anthraquinone patents. *Expert Opin. Ther. Pat.*, 25, 1053. <https://doi.org/10.1517/13543776.2015.1050793>
- [7] Khanal, P., Patil, B.M., Chand, J., Naaz, Y. (2020). Anthraquinone Derivatives as an Immune Booster and their Therapeutic Option Against COVID-19. *Nat. Prod. Bioprospect.*, 10(5), 325–335. <https://doi.org/10.1007/s13659-020-00260-2>
- [8] Enmozhi, S. K., Raja, K., Sebastine, I., Joseph, J. (2020). Andrographolide as a potential inhibitor of SARS- CoV-2 main protease: An in-silico approach, *J. Biomol. Struct. Dyn.*, 39(9), 3092-3098 doi: 10.1080/07391102.2020.1760136
- [9] Daina, A., Michielin, O., Zoete, V. (2017). Swiss ADME: a free web tool to evaluate pharmacokinetics, drug-likeness and medicinal chemistry friendliness of small molecules, *Sci. Rep.*, 7, 42717. <https://doi.org/10.1038/srep42717>
- [10] Meng, X. Y., Zhang, H. X., Mezei, M., Cui, M. (2011). Molecular docking: a powerful approach for structure-based drug discovery, *Curr. Comput Aid. Drug.*, 7, 146–157. <https://doi.org/10.2174/157340911795677602>
- [11] Forli, S., Huey, R., Pique, M. E., Sanner, M. F., Goodsell, D. S. Olson, A. J. (2016). Computational protein-ligand docking and virtual drug screening with the AutoDock suite, *Nature protocols*, 11, 905–919. <https://doi.org/10.1038/nprot.2016.051>
- [12] Hassan, N. M., Alhossary, A. A., Mu, Y. (2017). Protein-ligand blind docking using Quick Vina-w with Inter-Process spatio-temporal Integration, *Sci. Rep.*, 7, 15451. <https://doi.org/10.1038/s41598-017-15571-7>
- [13] Saeed, A., Ur-Rehman, S., Channar P. A. (2017). Jack bean urease inhibitors, and antioxidant activity based on palmitic acid derived 1-acyl-3-arylthioureas: Synthesis, kinetic mechanism and molecular docking studies, *Drug. Res.*, 67, 596–605. doi: 10.1055/s-0043-113832
- [14] Shupeniuk, V., Amaladoss, N., Sabadakh, O., Taras, T., Matkivsky M. (2021). Synthesis of 4-substituted primary aliphatic aminoanthraquinones and in silico studies. *Russ. J. Org. Chem.*, 57(4), 582–588. <https://doi.org/10.1134/S1070428021040126>
- [15] Shupeniuk, V., Taras, T., Sabadakh, O., Luchkevich, E., Kornii Y. (2020). Synthesis some 4-substituted 9,10-anthraquinones. *French-Ukrainian Journal of Chemistry.* 8(1), 58–65. <https://doi.org/10.17721/fujcV8I1P58-65>
- [16] Li, H.; Li, N.J.; Gu, H.W. (2010). Two different memory characteristics controlled by the film thickness of polymethacrylate containing pendant azobenzothiazole. *J. Phys. Chem. C*, 114, 6117. doi.org/10.1021/jp910772m
- [17] Baqi, Y., Muller, C.E. (2012). Efficient and mild deamination procedure for 1-aminoanthraquinones yielding a diverse library of novel derivatives with potential biological activity. *Tetrahedron Lett.*, 53, 6739. <https://doi.org/10.1016/j.tetlet.2012.09.011>
- [18] Shupeniuk, V., Taras, T., Sabadakh, O., Luchkevich, E., Matkivsky, M. (2021). Methods of synthesis of hydroxyanthraquinone derivatives and their biological activity. *Journal of Chemistry and Technologies*, 29(2). 219–231. doi: 10.15421/jchemtech.v29i2.225941